The redshift distribution of gravitational lenses revisited: Constraints on galaxy mass evolution

Eran O. Ofek[*][1,2], Hans-Walter Rix[2], Dan Maoz[1]

[1] *School of Physics and Astronomy and Wise Observatory, Tel Aviv University, Tel Aviv 69978, Israel*
[2] *Max-Planck-Institut für Astronomie, Königstuhl 17, D-69117 Heidelberg, Germany*

ABSTRACT

The redshifts of lens galaxies in known gravitational lens systems probe the volume distribution of lensing mass. Following earlier work by Kochanek, we re-derive the lens redshift probability distribution, allowing for mass and number density evolution of the lensing galaxies, and apply this test to a much enlarged sample of lens systems. From a literature survey of all known lenses, we have selected an unbiased sample of 15 lenses with complete redshift information. For a flat Universe and no lens evolution, we can only put an upper limit on the cosmological constant of $\Omega_\Lambda < 0.89$ at the 95% CL. $\Omega_\Lambda \approx 0.7$ and no evolution is consistent with the data. Allowing for evolution in an $\Omega_m = 0.3$, $\Omega_\Lambda = 0.7$ cosmology, we find that the best-fit evolution in σ_* (i.e., the characteristic velocity dispersion in a Schechter-like function) of early-type galaxies, in the redshift range $z \sim 0$ to 1, is $d \log [\sigma_*(z)]/dz = -0.10 \pm 0.06$. This is consistent with no evolution and implies that, at 95% CL, σ_* of early-type galaxies at $z \sim 1$ was at least 63% of its current value. Alternatively, if there is no mass evolution, a present-day value of $\sigma_* > 175$ km s^{-1} for elliptical galaxies is required (95% CL).

Key words: cosmology: gravitational lensing – galaxies: general:evolution:mass function – quasars: general

1 INTRODUCTION

A number of recent measurements all point to a cosmology dominated by dark energy. The power spectrum of fluctuations in the cosmic microwave background indicates a flat geometry (e.g., Bennett et al. 2003), while various measurements of the fraction of the closure density in matter lead to consistent values of $\Omega_m \approx 0.3$ (e.g., Turner 2002). Observations of high-redshift supernovae Ia (Riess et al. 1998; Perlmutter et al. 1999) imply that the fraction of the closure density in the form of a cosmological constant is $\Omega_\Lambda \approx 0.7$.

However, some results obtained from gravitational lensing statistics appear to be at odds with this picture. The incidence of lensing among optically-selected quasars, and their image-separation distribution, indicate $\Omega_\Lambda < 0.7$ at 95% confidence level (CL; Maoz & Rix 1993; Kochanek 1996). Similar studies of radio-selected sources (Falco, Kochanek, & Munoz 1998) also find, $\Omega_\Lambda < 0.73$ at the 95% CL. Chiba & Yoshii (1999) have recalculated the predicted lensing statistics, using revised values for the galaxy luminosity function parameters, and have argued that a Universe with $\Omega_\Lambda = 0.7$ is the most likely one. Kochanek et al. (1998)

defended their choice of luminosity function parameters as the one that is most consistent with the observed luminosities of lens galaxies. Recently, Chae et al. (2002) derived constraints on cosmological parameters from analysis of radio selected gravitational lenses from the Cosmic Lens All Sky Survey (CLASS). They find a best fit $\Omega_\Lambda = 0.7 \pm 0.2$ and constrain $\Omega_\Lambda > 0$ at 95% CL, assuming the most recent galaxy luminosity function parameters from the 2dF survey (Madgwick et al. 2002) and the Sloan Digital Sky Survey (SDSS; Blanton et al. 2001). Note that, contrary to previous lensing statistics studies, in Chae et al. (2002) the velocity dispersion associated with a galaxy of given luminosity was left as a free parameter, rather than being set by direct observations. Their best fit velocity dispersions have relatively low values, which result in low lensing cross sections. This may be the main reason why their analysis favors a relatively high value of Ω_Λ.

Rix et al. (1994) investigated the impact of hierarchical galaxy mergers on the statistics of gravitational lensing of distant sources. They showed that the *total* number of multiple-image lenses in a sample of potential sources is quite insensitive to mergers, but merging leads to a smaller mean separation of observed multiple images. Since merging does not reduce drastically the expected lensing frequency,

it cannot make Λ-dominated cosmologies compatible with the existing lensing observations (e.g., Maoz & Rix 1993). Malhotra, Rhoads, & Turner (1997) have suggested that small-separation lensing statistics can be reconciled with an Ω_Λ-dominated Universe by invoking dust in the lensing galaxies. The excess number of lensed quasars would then be hidden by extinction. Falco et al. (1999) found a mean extinction value of $\Delta E_{B-V} = 0.04$ (0.06) for lens galaxies in optically-selected (radio-selected) systems. They tentatively concluded that the derived total extinction in lenses accounts for the small differences in limits on Ω_Λ found from lensing studies of radio selected vs. optically-selected sources.

Another interesting statistic, that is the focus of this paper, was suggested by Kochanek (1992), and is based on the redshift of the lensing galaxy in known lens systems. Fukugita, Futamase, & Kasai (1990) already showed that the expected mean redshift of the deflector increases if Ω_Λ dominates over Ω_m, due to the large volume at high redshifts. Kochanek (1992) obtained a formula for the probability distribution of the lens-galaxy redshift given a source (e.g., quasar) redshift and the critical radius for lensing. The critical radius for lensing was calculated assuming galaxy lenses can be represented by singular isothermal spheres (SIS) that are isolated (i.e., the lensing is not affected by masses other than the lens galaxy). The Kochanek method is applied by comparing for each model (cosmology) the redshift of the known lens, z_l, with the redshift probability distribution of the lens galaxy given the image separation and the source redshift, z_s. Using a sample of four lenses, Kochanek (1992) found that the then-standard cosmologies (without a cosmological constant) are 5-10 times more probable than a flat cosmology with $\Omega_\Lambda \gtrsim 0.9$. Since the image separation is taken into account as a prior, this method is not affected by a bias resulting from the fact that larger separation lenses are more easily discovered. This advantage allows, in principle, to use almost all the known lenses, regardless of their method of discovery. In §3 we will discuss some exceptions.

Kochanek (1992) raised several questions and problems regarding his method: (i) How to deal with objects in which it is difficult to detect the lens directly - should one trust a tentative lens redshift based on absorption lines? (ii) Is an unevolving galaxy mass distribution justified? (iii) The lens system should not be selected based on the lens-galaxy redshift. For example, Q2237+0305 was discovered based on the quasar emission lines present in the spectra of a nearby galaxy. More examples of such objects, which may be found in the 2dF survey and the SDSS (e.g., Mortlock & Webster 2001), are naturally biased toward lens galaxies at low redshift; (iv) The method requires lenses produced by isolated galaxies. Otherwise, the image separations do not necessarily represent the lens mass, and indeed Kochanek removed from his sample objects that are influenced by clusters (e.g., Q0957+561).

The redshift distribution test was re-examined by Helbig & Kayser (1996), who compared the redshifts of six lensing galaxies with the probabilities predicted by different cosmological models. They assumed that there is no galaxy evolution, and that lens galaxies could not be detected beyond a certain magnitude m_{lim}. For each tested cosmological model, they truncated the redshift probability distribution beyond the redshift at which the lens galaxy would become too faint to have its redshift measured. They concluded that the method is not sensitive to cosmological parameters and in the foreseeable future it would probably not deliver interesting constraints. Kochanek (1996) argued, however, that the insensitivity found by Helbig & Kayser (1996) was an artifact of their statistics, due to the fact that they accounted only for lenses with known redshifts, while the fraction of the lenses with unmeasurable redshifts was neglected. The fraction of lens systems with measured redshifts is smaller in a Λ-dominated Universe. This is due to the higher lens redshifts for a given source redshift, combined with a much larger luminosity distance to a given redshift. In order to account for the selection effect introduced by the detectability of the lens galaxy, Kochanek (1996) took into account also lens systems for which the lens redshift was not measured. Using a total of eight systems (for four of which the lens redshift was available) he obtained, for a flat Universe, an upper limit of $\Omega_\Lambda < 0.9$ at the 95% CL.

Evolution of galaxy mass and number can complicate or bias an analysis of the lens redshift distribution. For example, a scarcity of lenses at higher redshifts may be due to evolution rather than to the smaller volume of a low Ω_Λ cosmology. In fact, there are observational indications for evolution in the galaxy luminosity function (e.g., Cohen 2002), and in the mass-to-light ratio (e.g., Keeton, Kochanek & Falco 1998; van Dokkum et al. 2001). Evolution of the lens luminosity function and K-corrections will also affect the value of m_{lim}. Cohen (2002) studied the galaxy evolution in the HDF-North region and concluded that, while the uncertainties are large, there is no sign of any substantial increase in the total mass in stars between $z = 1.05$ and $z = 0.25$.

Keeton (2002) has recently argued that lensing statistics predictions should be calibrated by counts of distant galaxies at $z \sim 0.5 - 1$ with properties similar to those of real lenses, and not by the local density of galaxies. Since distant-galaxy number counts depend themselves on cosmological volume, when one calibrates the lensing statistics by the number counts of distant galaxies, lensing statistics lose most of their sensitivity to cosmology. While in principle this is true, relating the observed light from high redshift galaxies, and the light evolution, to mass is not trivial. The advantage of lensing is that it probes mass distribution directly. Therefore, it is still a valid approach to compare the observed lensing statistics to the predictions of locally calibrated models of lensing populations, and to incorporate the mass and density evolution into the models. The mass evolution indicated by the lensing data can then be compared to the luminosity evolution implied by number counts, to gain insight both on cosmology and on the relation between mass and light.

The purpose of this paper is to revisit the question of the lens redshift distribution, its dependence on cosmology, and on the evolution of the lens population, for the larger sample of lensed quasars now available. In §2 we rederive Kochanek's formalism for the expected lens redshift distribution, but allow for number and mass evolution of the lens population. We also investigate the properties of the lens redshift distribution, and its sensitivity to different parameters. In order to define an unbiased sample, in §3 we conduct a literature survey for known gravitational lens system and list them (in an Appendix) with their basic parameters. In §4 we constrain the cosmological and mass-evolution pa-

rameter space. We discuss the results in §5, and give a short summary in §6.

2 CALCULATION OF THE LENS REDSHIFT DISTRIBUTION

2.1 Formalism

The differential optical depth to lensing per unit redshift is

$$\frac{d\tau}{dz} = n(\theta, z)(1+z)^3 S \frac{cdt}{dz}, \tag{1}$$

where $n(\theta, z)$ is the comoving number density of lenses that have critical angular radius for lensing θ at redshift z, S is the cross section for lensing, and cdt/dz is the proper distance interval.

We assume that the lens galaxies can be represented by a SIS potential. The SIS assumption is consistent with lens data, galaxy dynamics, and the X-ray emission from ellipticals (e.g., Fabbiano 1989; Rix et al. 1997; Treu & Koopmans 2002). Moreover, it is known that ellipticity in the lens galaxy mainly affects the relative numbers of two- and four-image lenses but not their overall measures (e.g., Keeton, Kochanek, & Seljak 1997). The critical radius (Einstein radius), and cross section, for lensing in a SIS potential are given by

$$\theta = 4\pi \left(\frac{\sigma}{c}\right)^2 \frac{D_{ls}}{D_s} f_E^2, \tag{2}$$

$$S = \pi \theta^2 D_l^2, \tag{3}$$

where D_l, D_s, and D_{ls} are the angular diameter distances between observer-lens, observer-source, and lens-source respectively (e.g., Fukugita et al. 1992). Note that in the SIS model, the separation between lensed images is always 2θ. Unless mentioned otherwise, we use "filled-beam" angular-diameter distances throughout this paper (as opposed to "empty-beam", [Dyer & Roeder 1972, 1973]). f_E is a free parameter that represents the relation between dark halos and their stellar component, as explained below.

The velocity dispersion σ_{DM} of the mass distribution and the observed stellar velocity dispersion σ need not be the same. Turner, Ostriker, & Gott (1984) argued that if elliptical galaxies have dark massive halos with more extended distributions than those of the visible stars, this dark material must necessarily have a greater velocity dispersion than the visible stars, and a factor of $(3/2)^{1/2}$ is required to give an r^{-2} density distribution (cf. Gott 1977). Kochanek (1992) adopted a parameter f_E that relates the dark-matter velocity dispersion σ_{DM} and the stellar velocity dispersion σ:

$$\sigma_{DM} = f_E \sigma. \tag{4}$$

Dynamical models by Franx (1993), and Kochanek (1993, 1994) demonstrated that the assumptions leading to the $(3/2)^{1/2}$ factor were incorrect. However, White & Davis (1996) argued based on X-ray observations that there is a strong indication that dark matter halos are dynamically hotter than the luminous stars. In our work, we have kept f_E as a free parameter, since it mimics the effects of: (i) systematic errors in the velocity-dispersion measurements of galaxies; (ii) large scale structures that change the typical separation between images (e.g., Martel, Premadi, &

Matzner 2002; see §3 below) - an increase of an arbitrary order F in the velocity dispersion is equivalent to an increase of F^2 in the typical separation θ (i.e., $\theta \propto \sigma^2$); (iii) softened isothermal sphere potentials which tend to decrease the typical image separations (e.g., Narayan & Bartelmann 1996), and could be represented by f_E somewhat smaller than 1. Kochanek (1996) already noted that small core radii will lead to only slight modifications of the tail of the lens redshift probability distribution. Moreover, there is no evidence for cores in lensing galaxies (e.g., Rusin & Ma 2001).

Martel et al. (2002) compared the distribution of image separations obtained from ray-tracing simulations in CDM models (Premadi et al. 2001), with analytical calculations. They found that the presence of the background matter tends to increase the image separations produced by lensing galaxies. However, they found this effect to be small, of order of 20% or less, and independent of the cosmological parameters (see also Bernstein & Fischer 1999). Bromley et al. (1998; see also Christlein 2000, Zabludoff & Mulchaey 1998) showed that the luminosity function of early type galaxies depends on environment and that richer environments tend to have a higher ratio of dwarf to giant galaxies than the field. Keeton, Christlein, & Zabludoff (2000) showed that this effect nearly (but not entirely) cancels the effect of the background matter, making the distribution of image separations essentially independent of environment. They predicted that lenses in groups have a mean image separation that is $\sim 0.2''$ smaller than that of lenses in the field. It is possible that all these factors can affect the images separation by up to ±20%. This can be mimicked by introducing $(0.8)^{1/2} < f_E < (1.2)^{1/2}$.

In order to derive the lens redshift probability we need the velocity-dispersion distribution function of galaxies. Such a function is not yet available directly, although it is expected that the SDSS and 2dF surveys, combined with a good understanding of aperture effects, will produce one soon. Instead, we start with the Schechter (1976) function,

$$n(L, z) = n_*(z) \left(\frac{L}{L_*(z)}\right)^\alpha \exp\left(-\frac{L}{L_*(z)}\right) \frac{dL}{L_*(z)}, \tag{5}$$

which provides a good description of the galaxy luminosity distribution. Using the SDSS data, Blanton et al. (2001) find that this function fits the number density of SDSS galaxies better than an alternative non-parametric model. In order to relate the luminosity to velocity dispersion, we use the Faber-Jackson relation (Faber & Jackson 1976; Kormendy & Djorgovski 1989; Bernardi et al. 2001) for early-type galaxies,

$$\frac{L}{L_*(z)} = \left(\frac{\sigma}{\sigma_*(z)}\right)^\gamma. \tag{6}$$

A similar relation (i.e., a Tully-Fisher relation), but with different σ_* and γ, is adopted for spiral galaxies.

From Equations 6 and 2 we obtain

$$\frac{L}{L_*(z)} = \left(\frac{\theta}{\theta_*(z)}\right)^{\gamma/2}, \quad \frac{dL}{L_*(z)} = \frac{\gamma}{2} \left(\frac{\theta}{\theta_*(z)}\right)^{\gamma/2} \frac{d\theta}{\theta}, \tag{7}$$

where

$$\theta_*(z) = 4\pi \left(\frac{\sigma_*(z)}{c}\right)^2 \frac{D_{ls}}{D_s} f_E^2. \tag{8}$$

In our rederivation of the lens redshift probability, we allow for evolution in n_*, L_*, and σ_*, with the following parametrization.

$$n_*(z) = n_* 10^{Pz}, \qquad (9)$$

$$L_*(z) = L_* 10^{Qz}, \qquad (10)$$

$$\sigma_*(z) = \sigma_* 10^{Uz}, \qquad (11)$$

where P, Q, and U are constants. U represent an evolution in the characteristic σ_*, of a Schechter-like "mass" function. Note that the definitions of P and Q are somewhat different than the ones used by Lin et al (1999). The definition of Q is the same as the one used by Cohen (2002). Throughout the paper we use n_*, L_*, σ_*, and θ_* to refer to the values at zero redshift, as opposed to $n_*(z)$, $L_*(z)$, $\sigma_*(z)$, and $\theta_*(z)$. Our parametrization is consistent with hierarchical galaxy merging. Mergers change only the position of the galaxies on the Faber-Jackson relation but not the basic shape of the relation. The scatter in the Faber-Jackson relation (e.g., Kormendy & Djorgovski 1989; Bernardi et al. 2001) can be taken into account using a Monte-Carlo simulation, as we discuss in §2.3.

Combining Equations 7 and 5, to obtain $n(\theta, z)$, and inserting $n(\theta, z)$, along with the evolution parametrization (Eq. 9, 10, and 11) into Eq. 1, we obtain the optical depth per unit redshift for a system with image separation 2θ and source redshift z_s,

$$
\begin{aligned}
\frac{d\tau}{dz}(\theta, z_s) = \quad & \tau_N 10^{z[-U\gamma(1+\alpha)+P]} f_E^2 \\
& \times (1+z)^3 \frac{D_{ls}}{D_s} D_l^2 \frac{cdt}{dz} \left(\frac{\theta}{\theta_*}\right)^{\frac{1}{2}\gamma(1+\alpha)+1} \\
& \times \exp\left[-\left(\frac{\theta}{\theta_*}\right)^{\frac{1}{2}\gamma} 10^{-zU\gamma}\right],
\end{aligned}
\qquad (12)
$$

where the normalization,

$$\tau_N = 4\pi^2 n_* \frac{\gamma}{2} \left(\frac{\sigma_*}{c}\right)^2. \qquad (13)$$

The lens light emission (as opposed to the lens mass) does not affect lensing, and therefore Q does not appear in Equation 12. For a given lens system, the dependence of $d\tau/dz$ on z gives the relative probability of finding the lens at different z's.

2.2   Choices for the Lens Parameters

Throughout this paper we adopt the Schechter function parameters for the b_J-band, found by Madgwick et al. (2002) from a sample of $75,000$ galaxies in the 2dF survey with median redshift of $z \sim 0.1$ (see also Blanton et al. 2001 for a similar result based on a smaller sample using the SDSS). We assume $\alpha = -0.54 \pm 0.01$ for early-type galaxies (ellipticals and S0) and $\alpha = -1.16 \pm 0.01$ as the average of late-type galaxies (weighted by their abundance). The relative abundance of early-type to late-type galaxies is adopted from the local density, as obtained by Madgwick et al. (2002), while the relative abundance of ellipticals (E) to S0 is obtained from Postman & Geller (1984; E:S0=39:61). We thus adopt $n_* = 1.46 \times 10^{-2}$; 0.61×10^{-2}; 0.39×10^{-2} h^3 Mpc^{-3} for spirals, S0s, and ellipticals, respectively. The typical uncertainties in these number are of order 5%. Note that these values are different from those used by Kochanek (1992, 1996). We do not incorporate evolution in α, as the redshift distribution test is not very sensitive to α (see §2.3).

	Spiral	S0	Elliptical
α	-1.16	-0.54	-0.54
n_* [h^3 Mpc^{-3}]	1.46×10^{-2}	0.61×10^{-2}	0.39×10^{-2}
γ	2.6	4.0	4.0
σ_* [km s^{-1}]	144	206	225

Table 1. The default parameters for the luminosity function and the Faber-Jackson relation.

A constant α is also justified by observations (Cohen 2002). For the Faber-Jackson relations, Bernardi et al. (2001) find $\gamma = 4.00, 3.91, 3.95, 3.92$ in the SDSS g, r, i, and z-bands, respectively, with about 5% error. The spectral dependence of the slope γ, is smaller than the typical scatter in the Faber-Jackson relation ($\sim 40\%$ in a ln-normal distribution; Bernardi et al. 2001). We therefore adopt $\gamma = 4.0$ for early-type galaxies. For the Tully-Fisher relation of spirals, we assume $\gamma = 2.6$, following Kochanek (1992). We take σ_* from Fukugita & Turner (1991), based on de Vaucouleurs & Olson (1982), and Efstathiou, Ellis, & Peterson (1988): $\sigma_* = 225$ km s^{-1} for ellipticals; $\sigma_* = 206$ km s^{-1} for S0s; and $\sigma_* = 144$ km s^{-1} for spirals. Note that M_* (the magnitude of a σ_* galaxy) given by Madgwick et al. (2001) and that given by Efstathiou et al. (1988) agree well, after applying the transformation between the b_J and B_T magnitude systems (i.e., $b_J = B_T + 0.29$).

Table 1 lists the default parameters we will assume in this paper. Unless mentioned otherwise, $f_E = 1$, $\Omega_m = 0.3$, $\Omega_\Lambda = 0.7$, $U = 0$, $P = 0$.

2.3   What Can Be Tested by the Lens Redshift Distribution

In this section we investigate the (generally complicated) behavior of $d\tau/dz(\theta, z_s)$ (Equation 12) as a function of the parameters involved in the problem. We also study the effect of the scatter in the Faber-Jackson relation on the lens redshift distribution.

Kochanek (1992) noted that the lens redshift distribution cuts off more sharply at high redshift than the total optical depth $d\tau/dz$ (i.e., Eq 12 integrated over all θ's), because the critical radius constraint introduces an exponential term from the Schechter function beyond the redshift at which an L_* galaxy is required to produce the observed separation. The sharp cutoff makes $d\tau/dz(\theta, z_s)$ a powerful tool. For example, the existence of relatively high redshift lenses, even in a small sample, can reject models in which such redshifts are beyond the cutoff in the lens-redshift distribution.

Figure 1 shows the lens redshift probability distribution for several different values of a given parameter, while keeping the rest of the parameters fixed. Unless otherwise noted, we use the morphological mix of galaxies with the default parameters described in §2.2, along with $z_s = 2$ and $2\theta = 1''$. Since it is not practical to scan all the parameter space shown in Figure 1, this figure can help us to isolate the parameters that have the most profound effect on the lens redshift distribution.

Evolution Parameters U and P: As seen in Fig 1-g the parameter U, which describes the evolution of the characteristic galaxy velocity dispersion, has a considerable ef-
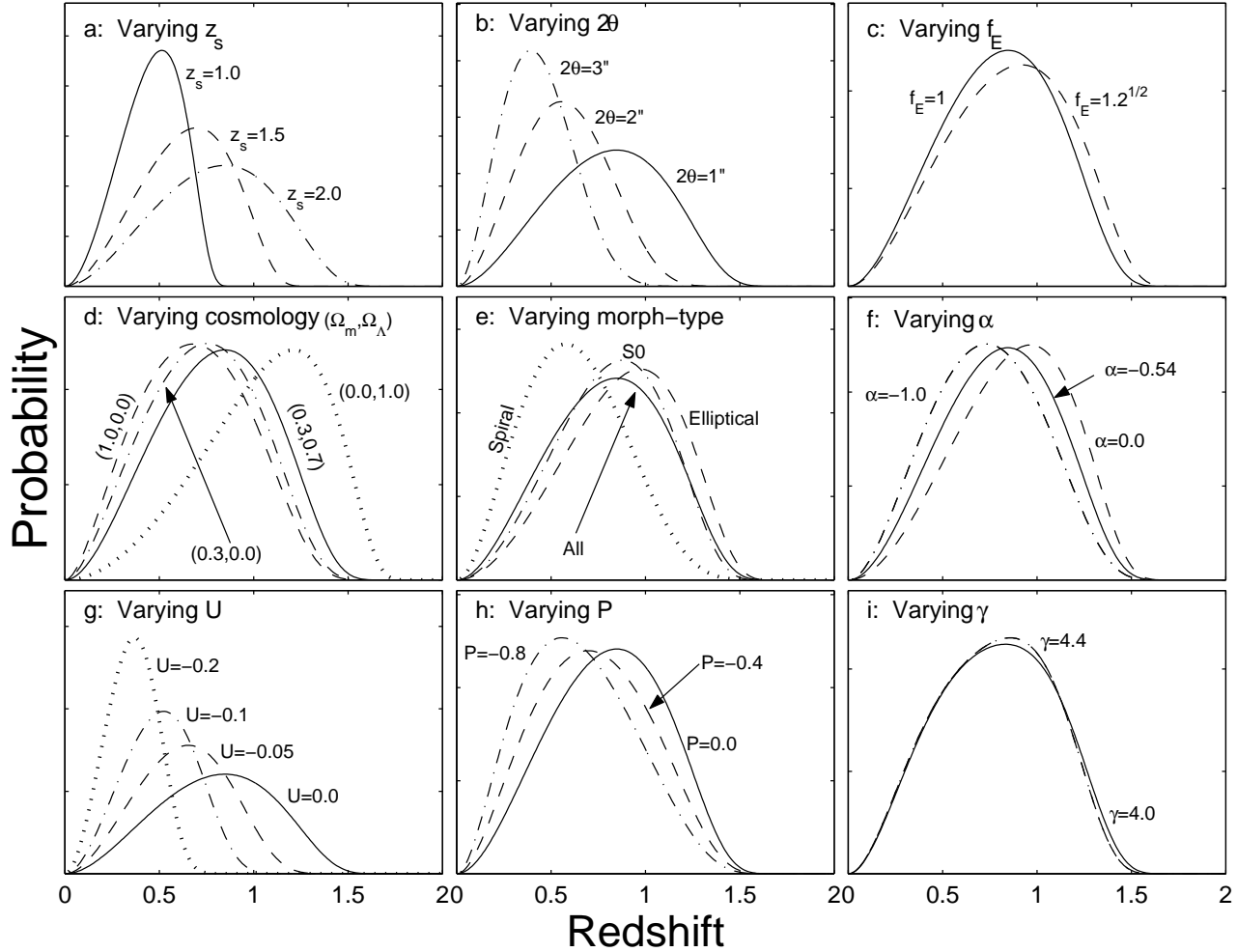
Figure 1. The lens redshift probability (normalized to one) density distribution as a function of redshift for various choices of parameters. The vertical axis is the probability in arbitrary units. In all panels, unless otherwise noted, we use the default parameters: $z_s = 2$, $2\theta = 1''$, $\Omega_m = 0.3$, $\Omega_\Lambda = 0.7$, $f_E = 1$, $U = 0$, $P = 0$, and the morphological mix with the parameters given in Table 1.

fect. Assuming $P \sim 0$, negative U decreases the most probable redshift of the lens z distribution, and makes the distribution narrower. This suggests that redshift evolution can impact the results considerably, and can therefore be constrained by the data. The effect of the number density evolution parameter, P (see Fig 1-h), is somewhat smaller, and mainly changes the most probable redshift, as opposed to U that affects also the cut-off redshift at which the lens-redshift probability goes to zero.

Cosmology: From Figure 1-d, it appears that the lens redshift distribution test in a flat Universe is sensitive to Ω_Λ mainly when $\Omega_\Lambda \gtrsim 0.8$.

Morphological type: It is well known (e.g., Maoz & Rix 1993) that almost all the contribution to lensing optical depth comes from early-type galaxies. Since the lensing galaxy type is not well constrained, in the analysis we will take it to be a mix of all the galaxy types [†]. As seen in Fig-

---

† Although several lens galaxies are clearly disk systems (e.g., B1600+434), even in those cases it is not clear whether they are S0's or later types.
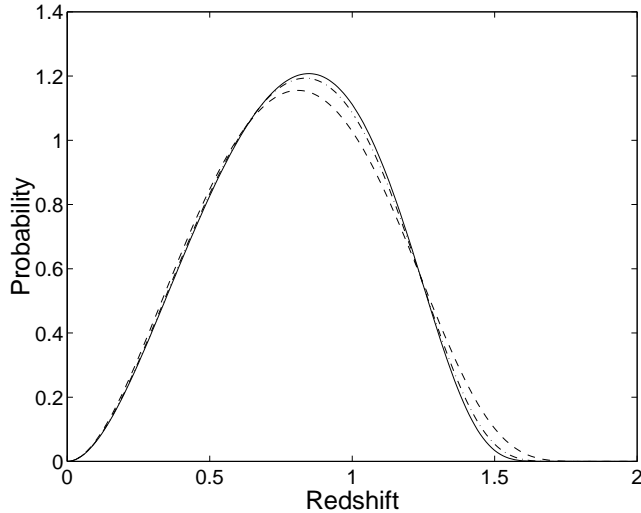
ure 1-e, as long as early-type galaxies dominate the lensing galaxy population, there will be no dramatic effect on the final results.

$\mathbf{f_E}$: As discussed in §2, the f_E parameter (Figure 1-c) can mimic the uncertainties in the relation between image separation and mass, or a systematic error in σ_*. Although the effect of complex environments on the image separation is not clear enough, it seems that in most cases it cannot change the image separation by more than 20% (see discussion in §1). Therefore, for reasonable values of $(0.8)^{1/2} < f_E < (1.2)^{1/2}$, f_E can somewhat affect the results of this work, but not as considerably as the mass evolution or a large cosmological constant. However, a systematic error of more than about 10% in σ_* can have some effect on the lens redshift distribution.

Angular diameter distance: We have tested the effect of the angular diameter distance formulae (filled-beam and empty-beam approximations) on the lens redshift distribution (not shown in Fig 1). Using empty-beam approximation somewhat decreases the typical lens redshift relative to the filled-beam approximation, but again, the effect is con-

Figure 2. The lens-redshift probability distribution for the default parameters, and $z_s = 2$ and $2\theta = 1''$ (solid line). The dotted-dashed and dashed lines were calculated using the same parameters, but for the mean of $10,000$ Monte-Carlo realizations with ln-normal scatter introduced to σ/σ_*, of 20% and 40% respectively.

siderably smaller than that of mass evolution or of a large cosmological constant.

γ: Even a 10% change in γ does not cause significant variations in the lens redshift distribution. Note that the effect of γ in Figure 1-i is tested only for $U = 0$, and its effect on the exponential term of Eq. 12 is therefore limited.

α: The effect of changing α is shown in Figure 1-f. Madgwick et al. (2002) give a 2% error on α. Changing α by 10% (not shown) has a negligible effect, even smaller then the effect of changing γ. Setting α to a completely different value (e.g., $\alpha = -1.1$; Efstathiou et al. 1988), somewhat shifts the peak of the lens-redshift probability distribution.

An important issue that needs to be considered is the scatter in the Faber-Jackson relation, which could alter the results. The observed scatter in the Faber-Jackson relation is about 40% in a ln-normal distribution (Bernardi et al. 2001). To study the effect of such scatter, we have performed Monte-Carlo simulations. In each realization we perturbed σ/σ_* by multiplying it by a factor randomly selected from a ln-normal distribution with a given standard deviation. We performed two sets of Monte-Carlo simulations with standard deviation of 20%, and 40%. For each set we calculated the lens-redshift probability, averaged over the realizations, as a function of redshift. Figure 2 shows the mean effect of the scatter in the Faber-Jackson relation on the lens-redshift probability distribution. The solid line is the unscattered lens-redshift probability distribution as a function of redshift for the default parameters. The dashed-dotted line is the same, but when 20% scatter is introduced to σ/σ_*, and the dashed line is for a 40% scatter. It is clear that the Faber-Jackson scatter makes the distribution somewhat broader. However, it does not change the distribution significantly. Note that using the lens redshift distribution function based on a velocity dispersion distribution function would overcome this problem.

Given the most probable values of the parameters, the

mass evolution U has the most important effect on the lens-redshift distribution. This is not surprising since U appears in the exponential term of Equation 12. Next in importance are the cosmological constant, the number density evolution, P, and f_E. In what follows, we therefore investigate the parameters found to be important to this problem, namely U, P, f_E, and Ω_Λ.

3   SAMPLE SELECTION

Using the lens redshift distribution of known lenses to constrain cosmological parameters and galaxy evolution requires a sample free of selection effects and biases. In Table A1, we have compiled a list of 71 galaxy lens systems we are aware of (July 2002) with their basic properties. The main source for this list is the CASTLES database[‡] (Munoz et al. 1999) that, at the time of writing, included 65 systems. We have added six additional systems discovered recently: FIRST J100424.9+122922 (Lacy et al. 2002); HS0810+2554 (Reimers et al. 2002); PMNJ0134-0931 (Winn 2002b); FIRST J0816+5003 (Lehár et al. 2001); HE0435-1223 (Wisotzki et al. 2002); PSS2322+1944 (Carilli et al. 2002).

There are several lens-system candidates that, although listed in the CASTLES database, are of uncertain nature, usually due to differences in the spectra of the supposed lensed images or the non-detection of a lensing galaxy. Rejection of these candidates based on the absence of a lensing galaxy is problematic. For example, a lensing galaxy in a real lens system may be undetected because it is distant and hence faint. Systematically rejecting such systems would bias the sample against detecting the effect of a cosmological constant. We therefore reject lens candidates only if their image spectra show pronounced differences. Based on this criterion, Q0252-3249 (Morgan et al. 2000) is probably not a real lens. In any event, this object has $z_s = 2.24$, and we will see below that even if it were a real lens system it would not enter our sample.

As mentioned above, some lens systems have been discovered based on the properties of the lens galaxy, thus preferring low-redshift lenses. On the other hand, it is difficult to detect lensed quasars for which the lens galaxy is nearby, based on quasar selection. After removing from our sample lens systems discovered based on galaxy properties, we therefore expect a bias against low-z lenses. In principle, we should correct for this bias by modifying the lens-redshift distribution. In practice, the probability for such lenses at $z \lesssim 0.1$ is very low anyway and we can safely ignore this correction. Lenses rejected based on their discovery method (i.e., lens-galaxy selected, as opposed to source selected) are: Q2237+0305 (Huchra et al. 1985); CFRS03.1077 (Crampton et al. 2002); FIRST J0816+5003 (Lehár et al. 2001). We have also rejected all the lens candidates discovered in the HST medium deep survey (Ratnatunga, Griffiths, & Ostrander 1999): HST14176+5226; HST12531-2914; HST14164+5215; HST15433+5352; HST01247+0532; HST01248+0531;   HST16302+8230;   HST16309+5215; HST12369+6212; HST18078+4600; and in the Hubble Deep

Fields:
HDFS2232509-603243 (Barkana, Blandford, & Hogg 1999). These lenses were selected based on their morphology (e.g., the detection of a possible lensing galaxy) and therefore, could introduce a bias. Rejecting all these lens systems does not introduces any bias, since we are effectively ignoring entire surveys. Furthermore, only two of these systems have complete redshift information, and as we will see below, their source redshift is too high to be included in our sample. In Column 10 of Table A1 these objects are marked "L".

There are several lens candidates (listed as binary quasars in the CASTLES database) whose nature is not clear (e.g., Q1634+267, Peng et al. 1999; Q2345+007, Small, Sargent, & Steidel 1997, Green et al. 2002). Even if these systems are real lenses, we reject them from our sample, since their separation is too large for galaxy lensing, and they could be affected by cluster-mass objects.

Kochanek (1996) accounted for systems with missing redshifts by considering the probability that one cannot detect the lens galaxy given the limiting magnitude to which a system has been probed. However, the lens galaxy brightness depends on galaxy luminosity evolution and this could complicate the analysis. In order to avoid this problem we have defined a sample that is source-redshift limited. We have selected all systems with $z_s < 2.1$ and image separations smaller than $4''$ (Sample I). This z_s selection criterion has several advantages: (i) Even for a de-Sitter Universe ($\Omega_\Lambda = 1$), the most probable redshift is < 1.2 and therefore we can probe the evolution factors within a similar redshift range to that studied by optical surveys (e.g., Cohen 2002); (ii) For $z_s < 2.1$ we can expect that the redshifts for most of the lenses have been measured, since they are not too high. However, selecting a limit (as we have) that is based on the largest z_s for which z_l is measured for most systems, is somewhat biased. For example, in a Λ-dominated Universe, the typical z_l will be higher and therefore the maximum z_s (for which the sample is complete) will be lower. To check for the robustness of the final results, we have defined a second sample (Sample II) for which the maximum z_s is 1.7.

The lens redshift information in the samples is not complete. There are three lens systems for which the lens redshift is not available yet. These are J0158-4325 (Morgan et al. 1999), HE0435-1223 (Wisotzki et al. 2002), and HS0810+2554 (Reimers et al. 2002). All three systems were discovered recently, and spectral observations *have not been attempted*. However, the lens galaxies are detectable and are actually quite bright ($R = 19.4$, $i = 18.1$, and $I \sim 19$, respectively) relative to other lens galaxies. Therefore, dropping these systems from our sample will not introduce a bias. For all but one of the lensing galaxies in samples I and II, the lens redshift has been measured spectroscopically. The exception is FBQ0951+2635, for which we have used the $BVRI$ photometry of Schechter et al. (1998), corrected for Galactic extinction (Schlegel, Finkbeiner, & Davis 1998), to calculate a photometric redshift by χ^2 minimization relative to galaxy spectral templates from Kinney et al. (1996). We find a photometric redshift of 0.23, 0.24, and 0.28, for Sb, S0 and E0 galaxy types, respectively. Kochanek et al. (2000) showed that early-type field galaxies with $0 < z < 1$, as represented by lens galaxies in lensed quasar systems, lie on the same fundamental plane as those in rich clusters at similar redshifts. They used this to estimate the "fundamental-

plane redshift" of lens galaxies by matching the lens galaxy effective radius, magnitude and velocity dispersion to the fundamental plane of rich clusters. The Kochanek et al. (2000) fundamental-plane redshift for FBQ0951+2635, although somewhat dependent on cosmology through the luminosity distance, is consistent ($z_l = 0.21 \pm 0.03$) with our photometric redshift. Based on these estimates, we have adopted, $z_l = 0.25$, for FBQ0951+2635. In §4 we check for the robustness of this assumption by changing the redshift of this object by ± 0.05. The lens system B2045+265 was excluded from all the samples, since its source redshift is most likely in error (see Fassnacht et al. 1999).

The image separation criterion of $4''$ was introduced in order to remove lenses that are influenced by complex environments (e.g., clusters). The separation is used as prior information in calculating the lens redshift probability for each system. Therefore, even if we reject a lens that has a large separation, only because its lens redshift is very low relative to the source redshift, this selection will not bias the experiment. On this basis we have removed Q0957+561, and RXJ0921+4529 from Samples I and II. To test for the robustness of this cut, we have defined Sample III, in which we have used sample I plus these two $\sim 6''$ separation lenses. Samples I, II, and III contain 15, 11, and 17 sources, respectively.

For six lenses in sample I for which an elliptical isothermal sphere plus shear model is available in the CASTLES database, the critical radius (θ) from the model is about half the observed image separation (or half the maximum separation in quadruple systems) to 10% accuracy or better. Therefore, we adopt half the image separation as representing the critical radius in all systems.

4 ANALYSIS

Figure 3 shows the lens redshift probability distribution, as calculated using Equation 12 with the default parameters, for each of the lenses in samples I, II, and III. In each panel the name of the lens along with its source redshift (z_s), lens redshift (z_l), and image separation (2θ) in arcseconds are listed. The actual lens redshift is marked by an arrow on the bottom axis.

Our statistical analysis is based on the maximum likelihood technique. For each lens system (i), given the model (described by Equation 12), we calculate the probability density $P_i(z_l|z_s, \theta; \mathbf{X})$, which is normalized to one, where $\mathbf{X}$ are the model parameters (e.g., Ω_Λ, U), and z_s and θ are priors. The log likelihood ($\ln \mathcal{L}$) as a function of $\mathbf{X}$ is given by

$$\ln \mathcal{L} = \sum_i \ln P_i. \qquad (14)$$

Testing one parameter at a time (i.e., X_j), the confidence interval (CI) within a given confidence limit (CL), is the region found below the peak of the log likelihood by 0.5, 2.0, and 3.3174, for 68%, 95%, and 99% CLs, respectively (e.g., Press et al. 1992).

Figure 4 shows $\ln \mathcal{L}$ for the full sample I. The dotted horizontal lines are the 68%, 95%, and 99% CLs, from top to bottom, respectively. From this figure we see that the most likely cosmological model (assuming no evolution) is
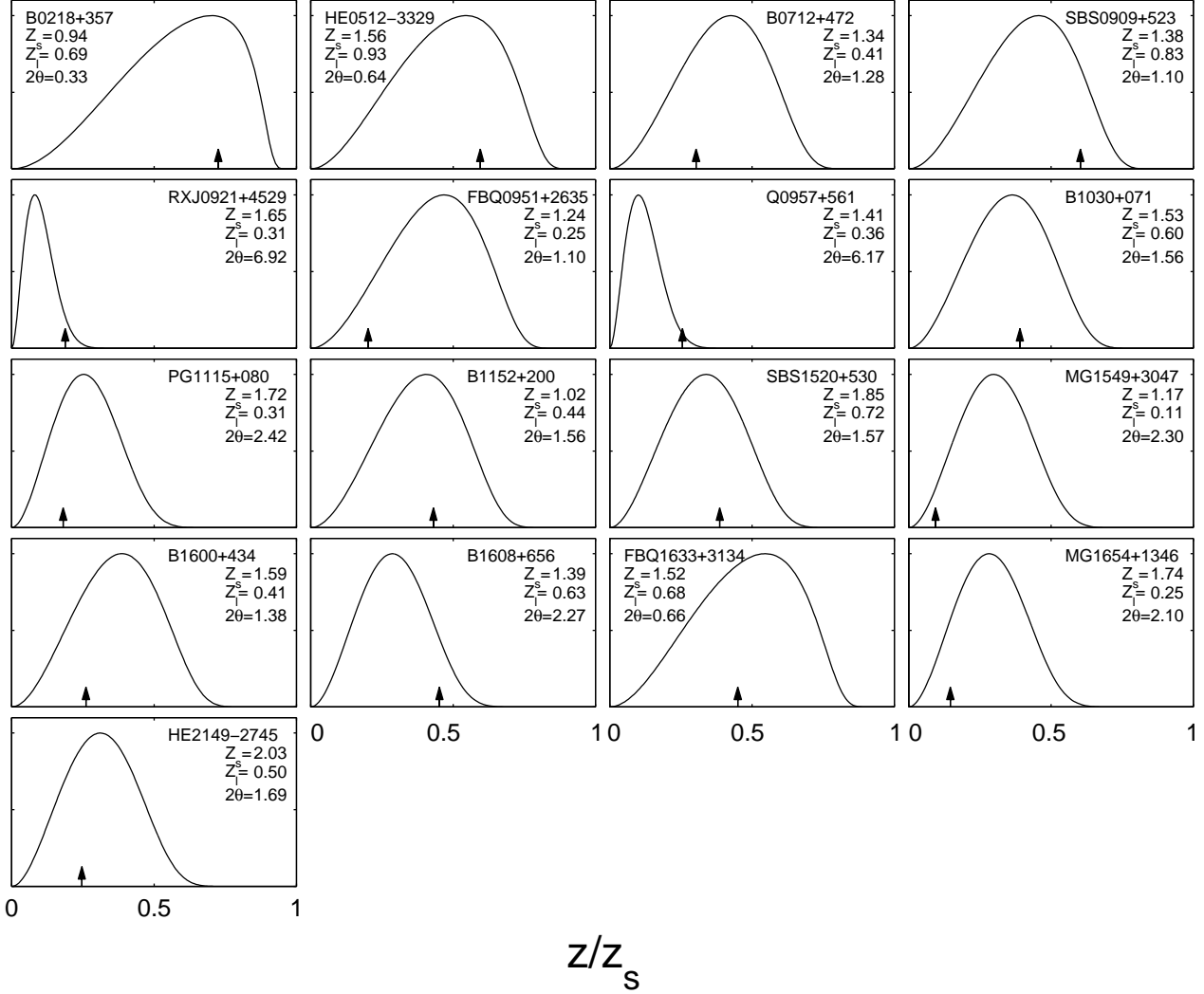
Figure 3. Lens redshift probability distributions calculated for morphological mix of galaxies with the default parameters (see §2.2), for each of the 17 lenses in samples I, II, and III. The vertical axis is the probability in arbitrary units. In each panel the name of the lens along with its source redshift (z_s), lens redshift (z_l) and image separation in arcseconds (2θ) are noted. The observed lens redshift is marked by an arrow on the bottom axis.

$\Omega_\Lambda = 0.36^{+0.35}_{-0.70}$, with upper limits $\Omega_\Lambda < 0.89$ at the 95% CL, and $\Omega_\Lambda < 0.95$ at the 99% CL.

The maximum-likelihood technique is not free of bias (i.e., the most likely value could be biased; e.g., Efron 1982; Shao & Tu 1995). To test the results for bias and possible outliers, we use the Quenouille-Tukey jackknife technique (e.g., Efron 1982; Efron & Tibshirani 1993). For a sample of N "observations", we remove one "observation" (i.e., one system) at a time, and calculate $\ln \mathcal{L}$ as a function of Ω_Λ, for the $N-1$ remaining observations. The jackknife estimate for the bias, B, in the parameter η (i.e., Ω_Λ) is given by $B = (N-1)(<\eta_i> -\eta)$. Where η is estimated using N observations, and η_i is the same, but using $N-1$ observations at a time, where i is the index of observation dropped. This bias should be subtracted from η to obtain the corrected η. We find a bias of about $\Delta\Omega_\Lambda \approx -0.2$. Taking into account the bias, the most probable $\Omega_\Lambda \approx 0.6$ is well within the 1σ error and therefore we will ignore the bias.

Sample II favors a somewhat larger $\Omega_\Lambda = 0.60^{+0.27}_{-0.60}$.

The higher Ω_Λ favored by sample II may be due to the z_s cut we introduced (see §3). However, the Ω_Λ values from the two samples are consistent within the uncertainty indicated by the likelihood ratios. Sample III favors an even higher cosmological constant, $\Omega_\Lambda = 0.77^{+0.13}_{-0.22}$ (1σ errors). This result is not surprising, since cluster-affected lenses which have large separation will tend to have lenses at redshifts higher than expected, assuming low Ω_Λ and ignoring the effect of the cluster. This will increase the derived value of the cosmological constant.

As noted in §3, the redshift of the FBQ0951+2635 lens is based on a photometric redshift. In order to test for the robustness of this datum, we have recalculated $\ln \mathcal{L}$ when perturbing the lens redshift within the plausible range of redshifts ($z_l = 0.25 \pm 0.05$; see §3), and have found that it has little effect.

Given a model, the maximum-likelihood technique gives information about the best fit parameters of the model. However, the technique does not give information on the ac-
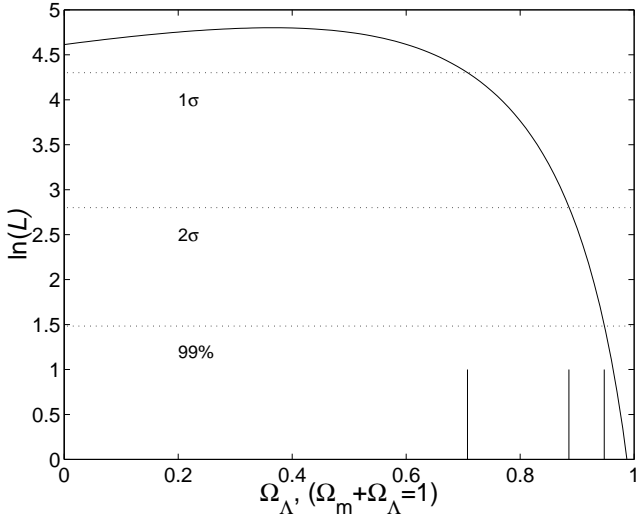
Figure 4. Likelihood plot for Sample I. The solid curve is the log of the likelihood as a function of Ω_Λ for $\Omega_m + \Omega_\Lambda = 1$. The rest of the parameters are the default ones. The dotted lines are the 1σ, 2σ and 99% CLs. The vertical lines on the bottom axis mark the points where $\ln \mathcal{L}$ crosses the dotted lines.

Figure 5. Likelihood contours in the U-P plane. The solid curves are the, 1σ, 2σ and 99% CL lines for sample I, where the plus sign mark the position of maximum likelihood. The dotted curves are these contours for sample II, for which the triangle marks the position of the maximum.

tual validity ("goodness of fit") of any model. To this end, we have performed a set of Monte-Carlo simulations. Given a set of model parameters, in each simulation we used the source redshift (z_s) and image separation (2θ) of the objects in sample I to generate a set of 1000 "sample I" realizations. Each realization contains 15 lens redshifts (like sample I). We then calculated the likelihood expectation value, and its distribution, as a function of Ω_Λ. We find that the likelihood expectation value is about 4.4 ± 1.1 (1σ errors), with some dependence on Ω_Λ, in good agreement with the maximum likelihood shown in Figure 4. We conclude that the lenses in sample I have redshifts consistent with the probability function given by Equation 12, and that our basic assumptions are probably valid.

Next, we set the cosmology to $\Omega_m = 0.3$, $\Omega_\Lambda = 0.7$, as found by Bennett et al. (2003), and maximize the likelihood for the evolution parameters. Note that the evolution parameters U and P are applied to all morphological types. As the cross section for spiral lensing is considerably smaller than for ellipticals, U and P effectively trace the evolution in early-type galaxies. Figure 5 shows the likelihood contours in the U-P plane. The solid curves are the 1σ, 2σ and 99% CL contours (for two degree of freedom, see Press et al. 1992) for sample I, where the plus sign marks the position of maximum likelihood. The dotted curves mark the same contours for sample II, for which the triangle marks the position of the maximum likelihood. We can see that both samples give consistent results. As expected, the lens redshift distribution is a better probe of U than of P. Marginalizing over P, Figure 6 shows $\ln \mathcal{L}$ as obtained by integrating $\mathcal{L}(P, U)$ over P (i.e., $\ln \int \mathcal{L}(P, U) dP$). In the absence of prior knowledge regarding P, we obtain $U = -0.10^{+0.06, +0.15, +0.23}_{-0.06, -0.10, -0.13}$, where the errors are for the 1σ, 2σ and 99%-CL CIs, respectively. Similarly, marginalizing over U, we get $P = +0.7^{+1.4}_{-1.2}$ (not shown). Finally, Figure 7 shows, for $\Omega_m = 0.3$, $\Omega_\Lambda = 0.7$, and no evolution in the number density of lenses ($P = 0$), the likelihood contours in the U-f_E plane. Assuming that
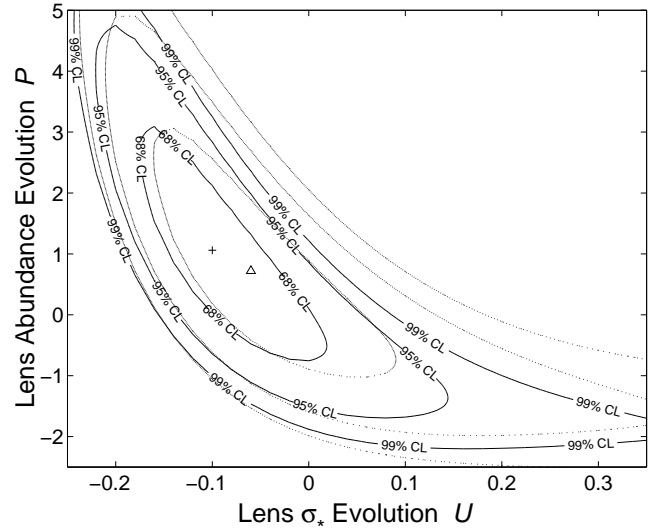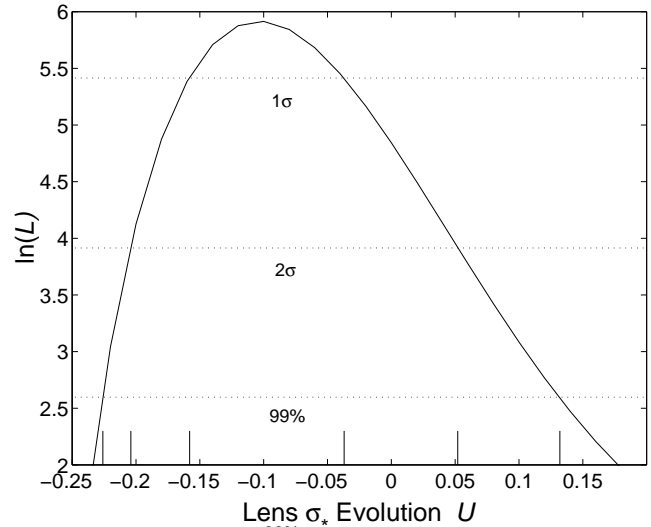

Figure 6. Marginalized likelihood as obtained by integrating $\mathcal{L}(P, U)$ over P (i.e., $\ln \int \mathcal{L}(P, U) dP$). Symbols as in Fig 4.

the dark-matter velocity dispersion and the stellar velocity dispersion are the same, and that large scale structures do not change considerably the image separations, then f_E represent a constant factor that multiplies the σ_*'s in Table 1. Thus, it mimics a systematic error in the "canonical" value of σ_* used in this paper. Assuming no evolution ($P = 0$, $U = 0$), we obtain a best fit $f_E = 0.90^{+0.08, +0.19, +0.28}_{-0.07, -0.12, -0.15}$ (1σ, 2σ and 99%-CL errors).

5 DISCUSSION

The lens redshift distribution test, like other cosmological tests, depends on assumptions, some of which may not be
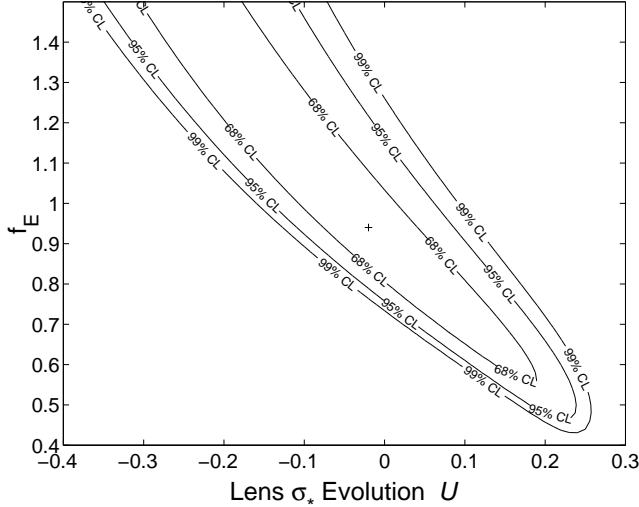
Figure 7. Likelihood contours in the U-f_E plane. The solid curves are the, 1σ, 2σ and 99% CL lines for sample I, where the plus sign mark the position of maximum likelihood.

correct. Based on the analysis we have conducted in §2.3, we would say that our most troubling assumption is that image separation truly represents the galaxy mass. Large scale structure can influence the image separation, and therefore we are probing some complex combination of galaxy mass and intervening structures and not the mass of the galaxy on its own. This is important as we use the "mass function" of galaxies to derive the lens redshift distribution. Our current knowledge suggests that in most cases, the image separation is not affected by more than 20% (see §2.1) by large scale structure.

Extinction can influence somewhat the number statistics of lenses, by lowering the observed number of optically selected lenses. Falco et al. (1999) found a mean value of $\Delta E_{B-V} = 0.05$ for lensed galaxies. The lens redshift distribution test is not influenced by dust, due to the fact that known lens systems are used and their image separations are taken as priors. However, for calculating the lens-redshift probability, we are using the observed mix of galaxy morphological types. Since spirals are more dusty, there could be a selection-induced lower fraction of spiral lenses relative to elliptical lenses, and this effect would lower the σ_*-evolution parameter, U, (or Ω_Λ) deduced by the lens redshift distribution method. However, the lens population is dominated by early-type galaxies by virtue of their larger mass. As shown in Figure 1, lowering the fraction of spiral lenses will not affect the predictions dramatically.

We showed that the lens redshift distribution test is sensitive to high values of the cosmological constant (e.g., $\Omega_\Lambda \gtrsim 0.8$). Using the lens redshift distribution, and assuming no evolution ($U = 0$, $P = 0$) and a flat Universe, the current sample puts an upper limit of $\Omega_\Lambda < 0.89$ at the 95% CL, and $\Omega_\Lambda < 0.95$ at the 99% CL. This is similar to the upper limit obtained by Kochanek (1996) for a much smaller sample, using the same method. Indeed, we find that the observations are consistent with the "concordance" value of $\Omega_\Lambda \approx 0.7$. Note, however, that this method with the current sample is still not a sensitive probe of Ω_Λ for $\Omega_\Lambda \lesssim 0.8$; our results are equally consistent with $\Omega_\Lambda = 0$.

We have shown that the lens redshift distribution is a sensitive probe of the velocity-dispersion evolution of early-type galaxies. This arises from the exponential dependence on the velocity-dispersion evolution parameter U in Equation 12. Assuming $\Omega_m = 0.3$, $\Omega_\Lambda = 0.7$ and no prior knowledge of U or P, then the best fit values are: $P = +0.7^{+1.4}_{-1.2}$ and $U = -0.10 \pm 0.06$. Our results apply to the redshift range ~ 0.1 to ~ 0.9. The lower limit is set by the median redshift of galaxies used to obtain the 2dF luminosity function (Madgwick et al. 2002) and the Faber-Jackson relation (Bernardi et al. 2001). The upper limit is set by the highest redshift lens in sample I ($z = 0.93$). Our results are consistent with no evolution. Positive U (mass increases with redshift) can probably be excluded as physically improbable. Our measurements are then useful for setting a lower limit on this "mass" evolution parameter. Negative U would mean that the typical characteristic velocity dispersion (in a Schechter-like function) σ_*, was lower in the past. Such evolution is expected in the hierarchical galaxy merging scenario, as the typical galaxy was less massive in the past. Our results imply that, at 95% CL, σ_* of early-type galaxies at $z \sim 1$ was at least 63% of its current value. As we have shown, the lens redshift distribution does not strongly constrain the number-density evolution P. If we take as a prior $P = -0.26$, as obtained by Im et al. (2002) and supported by Schade et al. (1999) from counts of early-type galaxies to $z \approx 1$, we see from Figure 5 that $U = -0.04^{+0.05, +0.10, +0.13}_{-0.04, -0.07, -0.09}$, where the errors are the 1σ, 2σ and 99% CL errors, respectively. This places a more severe limit on the allowed evolution in σ_*; at 95% CL, σ_* at $z \approx 1$ was at least 77% of its current value.

Most studies of galaxy evolution attempt to constrain the evolution of the light, or of the mass-to-light ratio defined by $(M/L)(z) = (M/L)_0 10^{Tz}$, rather than the mass evolution. The luminosity evolution, number evolution, and mass-to-light ratio evolution have been studied in various works that produced several estimates for the evolution parameters P, Q, and T. For example, Cohen (2002) studied the luminosity function of galaxies in the HDF-North region, in the redshift range 0 to 1.5. She found that galaxies with strong absorption lines become brighter with z ($Q \sim 0.6$ in all bands), while galaxies with detectable emission lines show a smaller change in L_*, with $Q \sim 0.3$. She also found that the comoving number density *and* stellar mass in galaxies is approximately constant out to $z \sim 1$, and with more uncertainty, to $z \sim 1.3$. Keeton, Kochanek, & Falco (1998) combined the photometry and lens modeling of 17 lens galaxies in the redshift range 0.1 to ~ 1. They found that the lens galaxy B-band mass-to-light ratio decreases with redshift with $T \approx -0.5 \pm 0.1$ (for $\Omega_m = 0.1$). In Table 2 we list these, and several other evolutionary studies of early-type galaxies, and their best fit parameters. The similar values of $-T$ and Q found by most studies, around 0.6, suggest considerable luminosity evolution with little mass evolution, consistent with our findings. Note that the evolution parameters listed in Table 2 are determined for early-type galaxies in different environments (field and clusters). Interestingly, the evolution parameters are similar.

In a recent paper, Davis, Huterer & Krauss (2002) use the CLASS and Jodrell-Very Large Array Astrometric Survey lensing statistics to constrain the characteristic velocity dispersion of elliptical galaxies. This is done using the joint

Reference	z_{max}	Parameters
van Dokkum et al. (1998)	0.83	$T \approx -0.45$
Keeton, Kochanek, & Falco (1998)	~ 1	$T \approx -0.5$
Lin et al. (1999)	0.55	$P = -0.7 \pm 0.2$
		$Q = 0.8 \pm 0.2$
van Dokkum et al. (2001)	0.55	$T = -0.59 \pm 0.15$
Cohen (2002)	~ 1	$Q \approx 0.6$
Rusin et al. (2002b)	~ 1	$T = -0.56 \pm 0.04$
Im et al. (2002)	~ 1	$Q = 0.8 \pm 0.3$
		$P = -0.26 \pm 0.20$

Table 2. Evolutionary parameters found using other methods. z_{max} is the maximum redshift for which the parameters were fitted. Since the parameters are cosmology dependent, we choose only works which assume a "standard" cosmology (i.e., $\Omega_m = 0.3$, $\Omega_\Lambda = 0.7$), or cosmologies that have luminosity distances that are not too different (e.g., $q_0 = 0.1$ as used by Lin et al. 1999, or $\Omega_0 = 0.1$ used by Keeton et al. 1998). Evolution in luminosity, number, and mass-to-light ratio are parameterized by Q, P, and T, respectively.

likelihood for the number of lenses, the redshift distribution of lensing galaxies, and the angular-separation distribution of lensed images. Their analysis gives 138 km s^{-1} $\leq$ $\sigma_* \leq 206$ km s^{-1} (95% CL). However, their lens-redshift distribution analysis include only the six out of 12 lenses in their sample for which redshift information is available. For a given image separation, lenses with higher redshift have higher masses. Therefore, failing to take into account the missing redshifts will bias σ_* toward lower values. Furthermore, the "canonical" value of σ_* (e.g., 225 km s^{-1} for ellipticals; Fukugita & Turner 1991) is measured at redshift zero, while the lensing analysis constrains σ_* at the mean redshift of the lenses. Therefore, it is hard to tell if the analysis by Chae et al. (2002) and Davis et al. (2002) is detecting evolution in σ_* or an error in the old value of σ_*. The mean lens-galaxy redshift of sample I is $\overline{z_l} = 0.54$. Our best fit value of $U = -0.10$ can be mimicked by a constant σ_* that is about 88% ($= 10^{U\overline{z_l}}$) of the local σ_* we have used in this work. However, we can see from Figure 7 that a σ_* that is $\lesssim 80\%$ of the values we have used in this paper (see Table 1), can be rejected since it would require positive evolution (U) at the 95% CL. Assuming no evolution ($U = 0$, $P = 0$), we have found that the most probable $f_E = 0.90^{+0.08,+0.19,+0.28}_{-0.07,-0.12,-0.15}$ (1σ, 2σ and 99%-CL errors). Therefore, a present-day value of $\sigma_* > 175$ km s^{-1} for elliptical galaxies is required (95% CL). This value is in agreement with a constant velocity dispersion as found by Chae et al. (2002), $\sigma_* = 198^{+53}_{-37}$ km s^{-1} for ellipticals. Note that Chae et al. (2002) use $\alpha = -1.0$, as opposed to $\alpha = -0.54$.

Thus, a constant value of $\sigma_* \approx 200$ km s^{-1} or a mildly evolving value that has approximately this average would explain most of the current lensing statistics data in an $\Omega_\Lambda = 0.7$ cosmology. Since lensing cross section is proportional to σ^4, such a value of σ_* may lower the lensing cross section in lens surveys by a large enough amount to explain the small number of observed lensed systems despite the large volume associated with a cosmological constant. At the same time our results show that such σ_* is still large enough to reproduce the observed redshift distribution of known lenses.

6 SUMMARY

We have compared the observed and predicted redshift distributions of lensing galaxies. Expanding upon the work of Kochanek (1992, 1996) we have used a much enlarged observational sample and incorporated possible mass and number density evolution of lens galaxies. The lens-redshift distribution in a flat Universe is sensitive to the large volume out to a given redshift in the presence of a large cosmological constant (i.e., $\Omega_\Lambda \gtrsim 0.8$), and especially to evolution of the characteristic velocity dispersion of the lensing population. The sensitivity of this test to velocity-dispersion evolution is unique, as it probes the total mass of stars and dark matter within ~ 10 kpc, without any assumptions on a possible bias factor between mass to light. We have explored the robustness of our inferences to various types of deviations from our basic assumptions, such as errors in the luminosity-function parameters, the lens model, and the scatter in the Faber-Jackson relation. Unless there are gross errors in our knowledge of these parameters, they have a small effect on our results.

There are now 71 lenses known in the literature and we have compiled their basic properties (Appendix A). From these, we have selected a sample of 15 lenses with separations smaller than $4''$ and source redshift $z_s < 2.1$, along with two other test samples. Assuming no mass evolution ($0 \lesssim z \lesssim 1$) of early-type galaxies, we can put an upper limit of $\Omega_\Lambda < 0.89$ at the 95% CL. On the other hand, assuming an $\Omega_m = 0.3$, $\Omega_\Lambda = 0.7$ cosmology we find that the best fit characteristic velocity dispersion (σ_*) and number evolution of early-type galaxies, in the range $z \sim 0$ to 1, are $d \log_{10} \sigma_*(z)/dz = -0.10 \pm 0.06$ and $d \log_{10} n_*(z)/dz = +0.7^{+1.4}_{-1.2}$. Our findings are consistent with no evolution in the early-type galaxy population and limit the allowed increase of the characteristic σ_* between $z \approx 1$ and the present. Finally, we have considered the influence of changing the estimate of the present-day value of σ_*. We find that a velocity dispersion that is $\lesssim 80\%$ of the standard value of σ_* would require positive velocity-dispersion evolution (i.e., galaxies were more massive in the past) at the 95% CL, and therefore can be rejected. A value of $\sigma_* \approx 200$ km s^{-1} for early-types, with no evolution out to $z \approx 1$, is consistent with our data. Such a value of σ_* could possibly also resolve the discrepancy between the results of previous lensing statistics studies and an $\Omega_\Lambda = 0.7$ cosmology.

REFERENCES

Augusto, P. et al. 2001, MNRAS, 326, 1007
Bernardi, M., et al., 2001, submitted to AJ, astro-ph/0110344

Barkana, R., Blandford, R., & Hogg, D. W. 1999, ApJL, 513, L91

Bernstein, G. & Fischer, P. 1999, AJ, 118, 14

Blanton, M. R. et al. 2001, AJ, 121, 2358

Bromley, B. C., Press, W. H., Lin, H., & Kirshner, R. P. 1998, ApJ, 505, 25

Burud, I. et al. 2002a, A&A, 383, 71

Burud, I. et al. 2002b, A&A, 391, 481

Carilli, C. L. et al. 2002, ApJ, 575, 145

Chae, K. 1999, ApJ, 524, 582

Chae, K.-H. et al. 2002, Physical Review Letters, 89, 151301

Chiba, M., Yoshii, Y. 1999, ApJ, 510, 42

Christlein, D. 2000, ApJ, 545, 145

Cohen, J. G. 2002, ApJ, 567, 672

Cohen, J.G., Lawrence, C.R., Blandford, R.D., 2002, Accepted for ApJ, astro-ph/0209457

Crampton, D., Schade, D., Hammer, F., Matzkin, A., Lilly, S. J., & Le Fèvre, O. 2002, ApJ, 570, 86

Faure, C., Courbin, F., Kneib, J. P., Alloin, D., Bolzonella, M., & Burud, I. 2002, A&A, 386, 69

Davis, A.N., Huterer, D., Krauss, L.M., 2002, submitted to MNRAS, astro-ph/0210494

Dyer, C. C. & Roeder, R. C. 1972, ApJL, 174, L115

Dyer, C. C. & Roeder, R. C. 1973, ApJL, 180, L31

Eisenhardt, P. R., Armus, L., Hogg, D. W., Soifer, B. T., Neugebauer, G., & Werner, M. W. 1996, ApJ, 461, 72

Efron, B., 1982, The Jackknife, the Bootstrap and Other Resampling Plans, The Society for Industrial and Applied Mathematics

Efron, B., Tibshirani, R.J., 1993, An introduction to the bootstrap, Monographs on statistics and applied probability 57, Chapman & Hall

Efstathiou, G., Ellis, R. S., & Peterson, B. A. 1988, MNRAS, 232, 431

Fabbiano, G. 1989, ARA&A, 27, 87

Faber, S. M. & Jackson, R. E. 1976, ApJ, 204, 668

Falco, E. E., Lehár, J., & Shapiro, I. I. 1997, AJ, 113, 540

Falco, E. E., Kochanek, C. S., & Munoz, J. A. 1998, ApJ, 494, 47

Falco, E. E. et al. 1999, ApJ, 523, 617

Fassnacht, C. D., Womble, D. S., Neugebauer, G., Browne, I. W. A., Readhead, A. C. S., Matthews, K., & Pearson, T. J. 1996, ApJL, 460, L103

Fassnacht, C. D. & Cohen, J. G. 1998, AJ, 115, 377

Fassnacht, C. D. et al. 1999, AJ, 117, 658

Fassnacht, C. D. & Lubin, L. M. 2002, AJ, 123, 627

Faure, C., Courbin, F., Kneib, J. P., Alloin, D., Bolzonella, M., & Burud, I. 2002, A&A, 386, 69

Franx, M. 1993, ApJL, 407, L5

Fukugita, M., Futamase, T., & Kasai, M. 1990, MNRAS, 246, 24P

Fukugita, M. & Turner, E. L. 1991, MNRAS, 253, 99

Fukugita, M., Futamase, T., Kasai, M., & Turner, E. L. 1992, ApJ, 393, 3

Goodrich, R. W., Miller, J. S., Martel, A., Cohen, M. H., Tran, H. D., Ogle, P. M., & Vermeulen, R. C. 1996, ApJL, 456, L9

Gott, J. R. 1977, ARA&A, 15, 235

Green, P. J. et al. 2002, ApJ, 571, 721

Gregg, M. D., Wisotzki, L., Becker, R. H., Maza, J. ;, Schechter, P. L., White, R. L., Brotherton, M. S., & Winn, J. N. 2000, AJ, 119, 2535

Gregg, M. D., Lacy, M., White, R. L., Glikman, E., Helfand, D., Becker, R. H., & Brotherton, M. S. 2002, ApJ, 564, 133

Hagen, H.-J. & Reimers, D. 2000, A&A, 357, L29

Hall, P.B., et al. 2002, accepted to ApJL, astro-ph/0207317

Helbig, P., Kayser, R., 1996, A&A, 308, 359

Hewett, P. C., Irwin, M. J., Foltz, C. B., Harding, M. E., Corrigan, R. T., Webster, R. L., & Dinshaw, N. 1994, AJ, 108, 1534

Huchra, J., Gorenstein, M., Kent, S., Shapiro, I., Smith, G., Horine, E., & Perley, R. 1985, AJ, 90, 691

Ibata, R. A., Lewis, G. F., Irwin, M. J., Lehár, J., & Totten, E. J. 1999, AJ, 118, 1922

Im, M. et al. 2002, ApJ, 571, 136

Keeton, C. R. & Kochanek, C. S. 1997, ApJ, 487, 42

Keeton, C. R., Kochanek, C. S., & Seljak, U. 1997, ApJ, 482, 604

Keeton, C. R., Kochanek, C. S., & Falco, E. E. 1998, ApJ, 509, 561

Keeton, C. R., Christlein, D., & Zabludoff, A. I. 2000, ApJ, 545, 129

Keeton, C. R. 2002, ApJL, 575, L1

Kinney, A. L., Calzetti, D., Bohlin, R. C., McQuade, K., Storchi-Bergmann, T., & Schmitt, H. R. 1996, ApJ, 467, 38

Kneib, J.-P., Alloin, D., Mellier, Y., Guilloteau, S., Barvainis, R., & Antonucci, R. 1998, A&A, 329, 827

Kneib, J., Cohen, J. G., & Hjorth, J. 2000, ApJ, 544, L35

Kobayashi, N., Terada, H., Goto, M., & Tokunaga, A. 2002, ApJ, 569, 676

Kochanek, C.S., 1992, ApJ, 384, 1

Kochanek, C.S., 1993, ApJ, 419, 12

Kochanek, C.S., 1994, ApJ, 436, 56

Kochanek, C.S, Falco, E.E., Impey, C.D., Lehár, J., McLeod, B.A., Rix, H.-W., 1998, in After the Dark Ages: When Galaxies Where Young (AIP), ed. S. Holt & E. Smith, p. 163

Kochanek, C. S. et al. 2000, ApJ, 543, 131

Koopmans, L. V. E. et al. 1999, MNRAS, 303, 727

Koopmans, L. ;. V. E. & Treu, T. 2002, ApJL, 568, L5

Kormendy, J. & Djorgovski, S. 1989, ARA&A, 27, 235

Lacy, M., Rawlings, S., & Serjeant, S. 1998, MNRAS, 299, 1220

Lacy, M., Gregg, M., Becker, R. H., White, R. L., Glikman, E., Helfand, D., & Winn, J. N. 2002, AJ, 123, 2925

Langston, G. I. et al. 1989, AJ, 97, 1283

Lehár, J., Langston, G. I., Silber, A., Lawrence, C. R., & Burke, B. F. 1993, AJ, 105, 847

Lehár, J. et al. 2000, ApJ, 536, 584

Lehár, J., Buchalter, A., McMahon, R. G., Kochanek, C. S., & Muxlow, T. W. B. 2001, ApJ, 547, 60

Lidman, C., Courbin, F., Kneib, J.-P., Golse, G., Castander, F., & Soucail, G. 2000, A&A, 364, L62

Lin, H., Yee, H. K. C., Carlberg, R. G., Morris, S. L., Sawicki, M., Patton, D. R., Wirth, G., & Shepherd, C. W. 1999, ApJ, 518, 533

Lubin, L. M., Fassnacht, C. D., Readhead, A. C. S., Blandford, R. D., & Kundić, T. 2000, AJ, 119, 451

Madgwick, D. S. et al. 2002, MNRAS, 333, 133

Magain, P., Surdej, J., Swings, J.-P., Borgeest, U., & Kayser, R. 1988, Nature, 334, 325

Malhotra, S., Rhoads, J.E., Turner, E.L. 1997,

Maoz, D., Rix, H.-W. 1993, ApJ, 416, 425

Marlow, D. R. et al. 1999, AJ, 118, 654

Marlow, D. R. et al. 2001, AJ, 121, 619

Martel, H., Premadi, P., & Matzner, R. 2002, ApJ, 570, 17

Morgan, N. D., Dressler, A., Maza, J., Schechter, P. L., Winn, J. N., 1999, AJ, 118, 1444

Morgan, N. D. et al. 2000, AJ, 119, 1083

Morgan, N. D., Becker, R. H., Gregg, M. D., Schechter, P. L., & White, R. L. 2001, AJ, 121, 611

Mortlock, D. J. & Webster, R. L. 2001, MNRAS, 321, 629

Munoz, J. A., Falco, E. E., Kochanek, C. S., Lehár, J., McLeod, B. A., Impey, C. D., Rix, H.-W., Peng, C. Y., 1999, Ap&SS, 263, 51

Muñoz, J. A. et al. 2001, ApJ, 546, 769

Myers, S. T. et al. 1999, AJ, 117, 2565

Narayan, R., & Bartelmann, M., 1996, In: "Lectures on Gravitational Lensing", astro-ph/9606001

O'Dea, C. P., Baum, S. A., Stanghellini, C., Dey, A., van Breugel, W., Deustua, S., & Smith, E. P. 1992, AJ, 104, 1320

Peebles, P.J.E., Ratra, B., 2002, astro-ph/0207347

Peng, C. Y. et al. 1999, ApJ, 524, 572

Perlmutter, S. et al. 1999, ApJ, 517, 565

Phillips, P.M., et al., 2000, 319, L7

Postman, M. & Geller, M. J. 1984, ApJ, 281, 95

Premadi, P., Martel, H., Matzner, R., & Futamase, T. 2001, ApJS, 135, 7

Press, W. H., Teukolsky, S. A., Vetterling, W. T., & Flannery, B. P. 1992, Cambridge: University Press, —c1992, 2nd ed.,

Ratnatunga, K.U., Griffiths, R.E., Ostrander, E.J., 1999, AJ, 117, 2010

Reimers, D., Hagen, H.-J., Baade, R., Lopez, S., & Tytler, D. 2002, A&A, 382, L26

Riess, A. G. et al. 1998, AJ, 116, 1009

Rix, H., Maoz, D., Turner, E. L., & Fukugita, M. 1994, ApJ, 435, 49

Rix, H., de Zeeuw, P. T., Cretton, N., van der Marel, R. P., & Carollo, C. M. 1997, ApJ, 488, 702

Rusin, D. & Ma, C. 2001, ApJL, 549, L33

Rusin, D. et al. 2001a, AJ, 122, 591

Rusin, D. et al. 2001b, ApJ, 557, 594

Rusin, D., Norbury, M., Biggs, A. D., Marlow, D. R., Jackson, N. J., Browne, I. W. A., Wilkinson, P. N., & Myers, S. T. 2002a, MNRAS, 330, 205

Rusin, D, et al. 2002b, accepted to ApJ, astro-ph/0211229

Schade, D. et al. 1999, ApJ, 525, 31

Schechter, P. 1976, ApJ, 203, 297

Schechter, P. L., Gregg, M. D., Becker, R. H., Helfand, D. J., & White, R. L. 1998, AJ, 115, 1371

Schlegel, D. J., Finkbeiner, D. P., & Davis, M. 1998, ApJ, 500, 525

Shao, J., Tu., P, 1995, in: The Jackknife and Bootstrap, Springer series in statistics, Springer Verlag

Siemiginowska, A., Bechtold, J., Aldcroft, T. L., McLeod, K. K., & Keeton, C. R. 1998, ApJ, 503, 118

Small, T. A., Sargent, W. L. W., & Steidel, C. C. 1997, AJ, 114, 2254

Surdej, J., Claeskens, J.-F., Remy, M., Refsdal, S., Pirenne, B., Prieto, A., & Vanderriest, C. 1997, A&A, 327, L1

Sykes, C. M. et al. 1998, MNRAS, 301, 310

Tonry, J. L. 1998, AJ, 115, 1

Tonry, J. L. & Kochanek, C. S. 1999, AJ, 117, 2034

Tonry, J. L. & Kochanek, C. S. 2000, AJ, 119, 1078

Treu, T., Koopmans, L. V. E., 2002, accepted to ApJ, astro-ph/0202342

Turner, M. S. 2002, ApJL, 576, L101

Turner, E.L., Ostriker, J.P., Gott III, R. 1984, ApJ, 284, 1

van Dokkum, P. G., Franx, M., Kelson, D. D., & Illingworth, G. D. 1998, ApJL, 504, L17

van Dokkum, P. G., Franx, M., Kelson, D. D., & Illingworth, G. D. 2001, ApJL, 553, L39

de Vaucouleurs, G. & Olson, D. W. 1982, ApJ, 256, 346

Walsh, D., Carswell, R. F., & Weymann, R. J. 1979, Nature, 279, 381

Warren, S.J., Hewett, P.C., Lewis, G.F., Moller, P., Iovino, A., Shaver, P.A., 1996, MNRAS, 278, 139

Wiklind, T. & Combes, F. 1995, A&A, 299, 382

Wiklind, T. & Combes, F. 1996, Nature, 379, 139

Winn, J. N. et al. 2000, AJ, 120, 2868

Winn, J. N., Hewitt, J. N., Patnaik, A. R., Schechter, P. L., Schommer, R. A., López, S., Maza, J. ;, & Wachter, S. 2001, AJ, 121, 1223

Winn, J. N. et al. 2002a, AJ, 123, 10

Winn, J. N., Lovell, J. E. J., Chen, H., Fletcher, A. ;., Hewitt, J. N., Patnaik, A. R., & Schechter, P. L. 2002b, ApJ, 564, 143

Wisotzki, L., Christlieb, N., Liu, M. C., Maza, J., Morgan, N. D., Schechter, P. L., 1999, A&A, 348, L41

Wisotzki, L., Schechter, P. L., Bradt, H. V., Heinmüller, J., & Reimers, D. 2002, A&A, 395, 17

White, R. E. & Davis, D. S. 1996, American Astronomical Society Meeting, 28, 1323

Zabludoff, A. I. & Mulchaey, J. S. 1998, ApJ, 496, 39

APPENDIX A: LIST OF KNOWN LENSES

Name (1)	R.A. (2)	Dec. (3)	z_s (4)	z_l (5)	separation (6)	mag_{lens} (7)	N_{im} (8)	Grade (9)	Sample (10)	Ref (11)
Q0047-2808	00:49:41.89	−27:52:25.7	3.595	0.4845	2.7	$V = 20.4$	4R	A		2,32
HST01247+0532	01:24:44.4	+03:52:00			2.17	$I = 21.9$	2	C	L	3
HST01248+0531	01:24:45.6	+03:51:06			0.738	$I = 22.6$	2	C	L	3
Q0142-100	01:45:16.5	−09:45:17	2.72	0.49	2.231	$R = 19.4$	2	A		32
B0128+437	01:31:13.405	+43:58:13.14			0.54		4	B		4
PMNJ0134-0931	01:34:35.73	−09:31:02.4	2.216	0.76451	0.7		5			24,25,48
J0158-4325	01:58:41.44	−43:25:04.20	1.29		1.22	$R = 19.4$	2	A		5
B0218+357	02:21:05.483	+35:56:13.78	0.944	0.685	0.33	$I = 20.1$	2R	A	I,II	51,52,62
HE0230-2130	02:32:33.1	−21:17:26	2.162	< 0.6	2.19	$V = 19.9$	4	A		6
Q0252-3249	02:52:57.90	−32:49:09.0	2.24		2.1	$R > 22.5$	2	B	N	8
CFRS03.1077	03:02:32.65	+00:06:00.2	2.941	0.938	2.1	$I = 20.4$	2R	B	L	9
MG0414+0534	04:14:37.73	+05:34:44.3	2.64	0.9584	2.12	$I = 21.3$	4R	A		10,14
HE0435-1223	04:38:14.90	−12:17:14.4	1.689	$\sim 0.4^p$	2.6	$i = 18.1$	4			43
HE0512-3329	05:14:10.78	−33:26:22.50	1.565	0.9313^a	0.644	$I = 17.6$	2	A	I,II	11
B0712+472	07:16:03.58	+47:08:50.0	1.339	0.406^b	1.28	$I = 19.5$	4	A	I,II	12
B0739+367	07:42:51.2	+36:34:43.7			0.54	$H = 19.0$	2	A		13
MG0751+2716	07:51:41.46	+27:16:31.35	3.200	0.3502^c	0.7	$I = 21.2$	R	A		14
HS0810+2554	08:13:31.29	+25:45:03.2	1.5		0.25	$I \sim 19$	2			7
FIRST J0816+5003	08:16:38.94	+50:04:06.4			1.8	$R = 19.2$			L	28
HS0818+1227	08:21:39.1	+12:17:29	3.115	0.39	2.55	$I = 18.8$	2	A		63
APM08279+5255	08:31:41.64	+52:45:17.5	3.911		0.378		3	A		15,16
SBS0909+523	09:13:01.05	+52:59:28.83	1.377	0.830	1.10	$I = 19.0$	2	A	I,II	27
RXJ0911+0551	09:11:27.50	+05:50:52.0	2.80	0.77^j	3.25	$H = 17.9$	4	A		30
RXJ0921+4529	09:21:12.81	+45:29:04.4	1.65	0.31^m	6.92	$I = 20.2$	2	B	III	35
FBQ0951+2635	09:51:22.57	+26:35:14.1	1.24	0.25^n	1.10	$I = 19.7$	2	A	I,II	53
BRI0952-0115	09:55:00.01	−01:30:05.0	4.50	0.41^o	0.99	$R = 22.1$	2	A		54
Q0957+561	10:01:20.78	+55:53:49.4	1.41	0.36^q	6.17	$I = 17.1$	3R	A	III	55
J100424.9+122922	10:04:24.872	+12:29:22.39	2.65	0.95^r	1.54		2			1
LBQS1009-0252	10:12:15.71	−03:07:02.0	2.74	0.88^s	1.53	$I = 22.0$	2	A		56
Q1017-207	10:17:24.13	−20:47:00.4	2.545	1.085^t	0.849	$I = 21.8$	2	A		37
FSC10214+4724	10:24:37.58	+47:09:07.2	2.286	0.914^y	1.59	$I = 20.4$	2R	A		57
B1030+071	10:33:34.08	+07:11:25.5	1.535	0.599	1.56	$I = 20.2$	2	A	I,II	12
HE1104-1805	11:06:33.45	−18:21:24.2	2.32	0.729	3.19	$I = 20.0$	2	A		46
PG1115+080	11:18:17.00	+07:45:57.7	1.72	0.311^x	2.42	$I = 18.9$	4	A	I	58
B1127+385	11:30:00.13	+38:12:03.1		$> 0.5^d$	0.701	$I = 22.7$	2	A		17
MG1131+0456	11:31:57.01	+04:55:50.6		0.844^f	2.1	$I = 21.2$	2R	A		19
B1152+200	11:55:18.3	+19:39:42.2	1.019	0.439	1.56	$I = 19.6$	2	A	I,II	36,45
Q1208+101	12:10:57.16	+09:54:25.6	3.80	1.1349^h	0.47	$H > 20$	2	B		26
HST12369+6212	12:36:49.0	+62:12:22			1.166	$I = 22.0$	2R	C	L	3
HST12531-2914	12:53:06.70	−29:14:30.0		0.63^z	1.09	$I = 21.8$	4	A	L	3
B1359+154	14:01:35.55	+15:13:25.6	3.235	$\approx 1^v$	1.7	$I = 22.7$	6	A		40
HST14113+5211	14:11:19.60	+52:11:29.0	2.811	0.465	2.26	$R = 20.5$	4	A	L	27
H1413+117	14:15:46.40	+11:29:41.4	2.558	w	1.35	$H = 18.6$	4	A		59
HST14164+5215	14:16:25.2	+52:14:31			2.18	$I = 20.8$	2	C	L	3
HST14176+5226	14:17:36.51	+52:26:40.0	3.40	0.81	3.25	$I = 19.7$	4	A	L	3
B1422+231	14:24:38.09	+22:56:00.6	3.62	0.339	1.28	$I = 19.6$	4R	A		58
SBS1520+530	15:21:44.83	+52:54:48.6	1.855	0.717^{ab}	1.568	$I = 20.2$	2	A	I	31,32
HST15433+5352	15:43:20.9	+53:51:52			1.176	$I = 20.2$	2R	C	L	3
MG1549+3047	15:49:12.37	+30:47:16.6	1.17^{aa}	0.11	2.3	$I = 16.7$	R	A	I,II	47
B1555+375	15:57:11.93	+37:21:35.9		u	0.42	$R = 25$	4	A	I,II	38
B1600+434	16:01:40.45	+43:16:47.8	1.589	0.4144	1.38	$I = 20.6$	2	A	I,II	12
B1608+656	16:09:13.96	+65:32:29.0	1.394	0.630	2.27	$I = 18.9$	4	A	I,II	39
HST16302+8230	16:30:12.9	+82:29:59			1.468	$I = 23.7$	2R	C	L	3
HST16309+5215	16:30:52.7	+82:30:12			0.760	$I = 20.2$	2R	C	L	3
PMNJ1632-0033	16:32:57.68	−00:33:02.05	3.424	1.0^e	1.47	$I = 23.1$	2R	B		18
FBQ1633+3134	16:33:48.99	+31:34:11.90	1.52	0.684^k	0.66	$H = 16.8$	2	B	I,II	33
MG1654+1346	16:54:41.83	+13:46:22.0	1.74	0.254	2.1	$I = 17.9$	R	A	III	50
HST18078+4600	18:07:46.7	+45:59:56			0.912	$I = 20.7$	2R	C	L	3
PKS1830-211	18:33:39.94	−21:03:39.7	2.51	0.886	0.99	$I = 21.4$	2R	A		60
PMNJ1838-3427	18:38:28.8	−34:27:33	2.78	0.31^g	1.00	$I = 21.4$	2R	A		20
B1933+507	19:34:30.95	+50:25:23.6	2.63	0.755	1.00	$I = 20.2$	10	A		41
B1938+666	19:38:25.19	+66:48:52.2		0.881	1.0	$I = 21.5$	R	A		19
PMNJ2004-1349	20:04:07.09	−13:49:31.1			1.13	$I = 21.9$	2R	A		21
MG2016+112	20:19:18.15	+11:27:08.3	3.27	1.004	3.26	$I = 22.0$	3R	A		42
B2045+265	20:47:20.35	+26:44:01.2	1.28	0.8673	2.2	$I = 21.2$	4	A		44
B2114+022	21:16:50.75	+02:25:46.9		0.32^i	1.3	$I = 18.6$	2+2	B		29
HE2149-2745	21:52:07.44	−27:31:50.2	2.03	0.50^l	1.69	$I = 19.6$	2	A	I,II	34,32

Name (1)	R.A. (2)	Dec. (3)	z_s (4)	z_l (5)	separation (6)	mag_{lens} (7)	N_{im} (8)	Grade (9)	Sample (10)	Ref (11)
HDFS2232509-603243	22:32:50.9	−60:32:43.0			0.9	$V = 22$	4?R	C	L	23
Q2237+0305	22:40:30.34	+03:21:28.8	1.695	0.0394	1.82	$I = 14.2$	4	A	L	49
B2319+052	23:21:40.8	+05:27:36.4		0.624	1.36	$H = 18.2$	2	A		22,27
PSS2322+1944	23:22:07.2	+19:44:23	4.12		1.5		2	B		61

Table A1. The columns are: (1) lens name; (2) R.A. [h:m:s], J2000.0; (3) Dec. [d:m:s], J2000.0; (4) source redshift, z_s; (5) lens redshift, z_l; (6) image separation in arcseconds, 2θ; (7) lens magnitude; (8) Number of images, R for ring; (9) Grade for the likelihood that the object is a lens, as adopted from the CASTLES database: A=I'd bet my life, B=I'd bet your life, and C=I'd bet your life and you should worry; (10) sample: L-lens was discovered based on the lens-properties (rather than the source), I- Sample I in this paper, II- Sample II in this paper, III-additional objects to those in Sample I, that are found in sample III; (11) References.
List of references:

1 - Lacy et al. (2002); 2 - Warren et al. (1996); 3 - Ratnatunga, Griffiths, & Ostrander (1999); 4 - Phillips et al. (2000); 5 - Morgan et al. (1999); 6 - Wisotzki et al. (1999); 7 - Reimers et al. (2002); 8 - Morgan et al. (2000); 9 - Crampton et al. (2002); 10 - Falco, Lehár, & Shapiro (1997); 11 - Gregg et al. (2000); 12 - Fassnacht & Cohen (1998); 13 - Marlow et al. (2001); 14 - Tonry & Kochanek (1999); 15 - Ibata et al. (1999); 16 - Kobayashi et al. (2002); 17 - Koopmans et al. (1999); 18 - Winn et al. (2002a); 19 - Tonry & Kochanek (2000); 20 - Winn et al. (2000); 21 - Winn et al. (2001); 22 - Rusin et al. (2001a); 23 - Barkana, Blandford, & Hogg (1999); 24 - Winn et al. (2002b); 25 - Gregg et al. (2002); 26 - Siemiginowska et al. (1998); 27 - Lubin et al. (2000); 28 - Lehár et al. (2001); 29 - Augusto et al. (2001); 30 - Kneib, Cohen, & Hjorth (2000); 31 - Burud et al. (2002b); 32 - Kochanek et al. (2000); 33 - Morgan et al. (2001); 34 - Burud et al. (2002a); 35 - Muñoz et al. (2001); 36 - Rusin et al. (2002a); 37 - Surdej et al. (1997); 38 - Marlow et al. (1999); 39 - Fassnacht et al. (1996); 40 - Rusin et al. (2001b); 41 - Sykes et al. (1998); 42 - Koopmans & Treu (2002); 43 - Wisotzki et al. (2002) ; 44 - Fassnacht et al. (1999); 45 - Myers et al. (1999); 46 - Lidman et al. (2000); 47 - Lehár et al. (1993); 48 - Hall et al. (2002); 49 - Huchra et al. (1985); 50 - Langston et al. (1989); 51 - O'Dea et al. (1992); 52 - Wiklind & Combes (1995); 53 - Schechter et al. (1998); 54 - Lehár et al. (2000); 55 - Walsh, Carswell, & Weymann (1979); 56 - Hewett et al. (1994); 57 - Eisenhardt et al. (1996); 58 - Tonry (1998); 59 - Magain et al. (1988); 60 - Wiklind & Combes (1996); 61 - Carilli et al. (2002); 62 - Cohen, Lawrence, & Blandford (2002); 63 - Hagen & Reimers (2000)

Notes:
a - Based on absorption line spectrum (Gregg et al. 2000).
b - Associated with a group at $z = 0.29$ and virial mass of ~ 300 km s^{-1} (Fassnacht & Lubin 2002).
c - Associated with a small group and possibly a second group at $z = 0.52$ (Tonry & Kochanek 1999).
d - Two late-type lensing galaxies (Koopmans et al. 1999).
e - Redshift is based on the Kochanek et al. (2000) method in which one requires that the galaxy properties be consistent with the passively evolving fundamental plane of early-type galaxies (Winn et al. 2002a).
f - Evidence for a foreground group of galaxies at $z = 0.34$ (Tonry & Kochanek 2000).
g - Redshift is based on the Kochanek et al. (2000) fundamental-plane method, plus the possible identification of [OIII] in emission (Winn et al. 2002b).
h - The most probable redshift is of an Mg II absorber at $z = 1.1349$ (Siemiginowska et al. 1998).
i - Complex lens, probably by two galaxies at $z = 0.3157$ and $z = 0.5883$ (Augusto et al. 2001).
j - Massive cluster at $z = 0.769$ with $\sigma \sim 840$ km s^{-1} (Kneib, Cohen, & Hjorth 2000).
k - Spectral observations reveal a rich metal-line absorption system consisting of a strong Mg II doublet and associated Fe I and Fe II absorption features, all at an intervening redshift of $z = 0.684$, suggestive of a lensing galaxy (Morgan et al. 2001).
l - By cross correlating the spectrum with galaxy templates, Burud et al. (2002a) obtain a tentative redshift estimate of $z = 0.50$, in agreement with the fundamental-plane method estimate (Kochanek et al. 2000).
m - Possibly a member of an X-ray cluster ($z = 0.32$) centered on the field (Muñoz et al. 2001).
n - Based on photometric redshift (this paper). The fundamental-plane method (Kochanek et al. 2000) gives $z_l = 0.21 \pm 0.03$.
o - $z_l = 0.41 \pm 0.05$ is based on Kochanek et al. (2000) fundamental-plane method.
p - Based on lensing galaxy colors $z = 0.4 \pm 0.1$ (Wisotzki et al. 2002).
q - Cluster at $z = 0.36$ (e.g., Chae 1999).
r - Based on the probable identification of the lens galaxy 4000Åbreak in the quasar spectra (Lacy et al. 2002).
s - Based on the fundamental-plane method (Kochanek et al. 2000) $z = 0.88 \pm 0.07$.
t - Absorption lines at $z = 2.344$ and MgII absorption at $z = 1.085$ (Surdej et al. 1997). Kochanek et al. (2000) based on the fundamental-plane method give $z = 0.78 \pm 0.07$. Therefore, we have adopted $z = 1.085$.
u - Marlow et al. (1999) argue that the lens galaxy is sub-L_*, so it has $z > 0.5$, or is highly reddened.
v - Lensing by a compact group of three $z \approx 1$ galaxies (Rusin et al. 2001b).
w - Possible cluster at $z \sim 1.7$ (Kneib et al. 1998).
x - Keeton & Kochanek (1997) find that the lens time-delay cannot be fit by an isolated lens galaxy, but that it can be well fitted by including a perturbation from the nearby group of galaxies. Tonry (1998) measures the group velocity dispersion of 330 km s^{-1}.
y - Eisenhardt et al. (1996) estimate the lens-galaxy redshift as $z = 0.9 \pm 0.3$. Goodrich et al. (1996) find strong evidence for MgII absorption at $z = 1.316$ in the spectrum of the QSO and weaker evidence for a possible continuum and absorption system at $z = 0.893$. Lacy, Rawlings, & Serjeant (1998) identify an Hα emission line with $z = 0.914$. The Kochanek et al. (2000) fundamental plane method gives $z = 0.78 \pm 0.05$.
z - Based on the Kochanek et al. (2000) fundamental plane method.
aa - L. Koopmans and T. Treu, private communication (radio ring detected in radio).
ab - Excess of galaxies at $z \sim 0.9$ (Faure et al. 2002).